# On the Role of Sea Surface Temperature Gradients in Forcing Low-Level Winds and Convergence in the Tropics

RICHARD S. LINDZEN AND SUMANT NIGAM

*Department of Earth, Atmospheric and Planetary Sciences, Massachusetts Institute of Technology, Cambridge, MA 02139*

(Manuscript received 20 August 1986, in final form 2 March 1987)

ABSTRACT

We examine the importance of pressure gradients due to surface temperature gradients to low-level ($p \geq 700$ mb) flow and covergence in the tropics over time scales $\geq 1$ month. The latter plays a crucial role in determining the distribution of cumulonimbus convection and rainfall.

Our approach is to consider a simple one-layer model of the trade cumulus boundary layer wherein surface temperature gradients are mixed vertically—consistent with ECMWF analyzed data. The top of the layer is taken at 700 mb. The influence from higher levels is intentionally suppressed by setting horizontal pressure gradients and frictional stresses to zero at the top of the layer. Horizontal convergence within the layer is taken up by cumulonimbus mass flux. However, the development of the cumulonimbus mass flux is associated with a short relaxation time [O(½ hr)] (roughly the development time for such convection). During this short time, horizontal convergence acts to redistribute mass so as to reduce horizontal pressure gradients. This effect proves important in the immediate neighborhood of the equator.

Our results show that flows forced directly by surface temperature are often comparable to observed low-level flows in both magnitude and distribution.

## 1. Introduction

There is considerable observational evidence (Cornejo-Garrido and Stone, 1977; Ramage and Hori, 1981; Rasmussen and Carpenter, 1982; Horel, 1982; Liebman and Hartmann, 1982) that precipitation anomalies in the tropics are closely associated with anomalies in sea surface temperature. Modeling studies (Shukla and Wallace, 1983; Stone and Chervin, 1984) confirm that precipitation anomalies are primarily associated with anomalous low-level moisture convergence rather than anomalies in evaporation. The purpose of the present paper is to determine the contribution of those pressure gradients directly produced by SST variations to the production of low-level convergence.

It is frequently assumed that the flow generated by the latent heat release in cumulus towers is an important component of the low-level convergence, and that the resulting moisture convergence below the detrainment level of the trade-cumuli (trade inversion) is largely proportional to the amount of cumulus convection and rainfall. This picture is, of course, at the heart of CISK (Charney and Eliassen, 1964; Kuo, 1965; Ooyama, 1969). However, even when CISK is not effective, the low-level convergence forced by cumulus heating is important. For example, it is invoked in most extant models of the El Niño (Zebiak, 1982). Nevertheless, whether the circulation driven by latent heat release in the mid- and upper tropical troposphere can actually produce enough low-level ($p > 700$ mb) moisture flux convergence to maintain itself is not clear. Gill's (1980) model, usually used in these implementations is, of necessity, tuned by the choice of damping parameters, and highly dependent on an artificial lid. As such, it cannot be used to settle this question. (We discuss Gill's model further in section 3.) The work of Schneider and Lindzen (1977), Schneider (1977), Stevens et al. (1977) and Stevens and Lindzen (1978) suggests that the flows generated by cumulus heating do not contribute effectively to low-level convergence (at least for time scales > 1 week) because the cumulus heating peaks in the upper troposphere and the forced motions decay away from the heating maximum. For zonally symmetric circulations, Schneider (1977) showed that the position of the ITCZ was determined largely by the surface temperature field.

Apart from the possible contribution of flows generated by latent heat release aloft to low-level convergence, there must also be contributions forced by low-level barotropic instability and by surface temperature gradients. There is little agreement at present as to what the most important contributor to moisture convergence is—assuming, of course, that any of the above is dominant. There is some evidence that barotropic instability is only of importance when the unstable shears are in the lower troposphere (Lindzen et al., 1982; Burpee and Reed, 1982); such situations are important but not universal. When such low-level instability is absent and/or when the interest is in the time-

mean flow, the competition is between the low-level convergence generated by cumulus heating (of the middle and upper troposphere) and that generated by surface temperature gradients. In this paper we determine the contribution of the surface temperature gradient driven flow to the observed low-level tropical convergence field.

To the best of our knowledge, no such explicit determination has yet been made. Most existing models have focused on the response to cumulus heating (Webster, 1972; Gill, 1980; Geisler, 1981; Zebiak, 1982; Rosenlof et al., 1986) presumably because latent heating is large in the tropics while temperature gradients are small. However, as is well known, small gradients can be very important in the tropics.

It has been pointed out by Riehl (1979), Lindzen (1981), Sarachik (1985) and others that the lower troposphere over the tropical oceans can be efficiently mixed in the vertical due to buoyant convection forced by surface evaporation. Such mixing is limited in the vertical by a trade wind inversion located at a height of 2 to 3 km; the inversion results from a balance between large scale subsidence and penetrative convection forced by surface buoyancy fluxes, and serves to isolate the relatively well-mixed trade cumulus boundary layer from the atmosphere above this level. Such a well-mixed layer and an accompanying inversion have been identified in the tropical Atlantic during the ATEX (Atlantic Tropical Experiment, 1974; Augstein et al., 1974) expedition; in the Pacific, a similar structure of the tropical lower troposphere has been observed/deduced (Neiburger et al., 1961; Riehl, 1979) in the "data-rich" northeastern sector that includes the California–Hawaii air–sea routes. Such an inversion is not easily identified in conventional coarse observations, but the underlying physics is common throughout the tropics and we will assume that something akin to the trade inversion must occur wherever, in the tropics, we have significant surface evaporation. It should be noted that current thinking differs from the earlier view that the trade inversion was an advected feature. Time scales based on penetrative convections are much faster than advective time scales (Betts, 1973; Sarachik, 1985). It is clear from these studies that the trade inversion would form in the absence of advection though advection may have some modest influence (Albrecht et al., 1979).

If the tropical lower troposphere is indeed relatively well mixed in the vertical, one would expect horizontal gradients of temperature (or virtual temperature) beneath the trade inversion (usually between the 850 and 700 mb levels) to bear sustantial resemblance to their surface pattern. ECMWF (European Centre for Medium Range Weather Forecasts) analyzed FGGE (First GARP Global Experiment) data [as archived at NASA's Goddard Laboratory for Atmospheres (GLA)] are available at 1000, 850, 700 and 500 mb; we check if the *analyzed* temperature fields at these levels exhibit any vertical correlation. That the analyzed *eddy* (where eddy is the departure from the average over all longitudes) temperature field is vertically correlated in the lower troposphere is apparent from Fig. 1 which shows the horizontal gradients of the eddy virtual temperature field at the 1000, 850 and 700 mb levels over the tropical Pacific during the northern summer (JJA); this figure is produced from a smoothed version (R15, rhomboidal truncation at 15) of the ECMWF analyzed FGGE dataset. Over the tropical Pacific Ocean, the meridional gradients are much larger than the zonal gradients even though the western Pacific is warmer than the eastern Pacific by as much as 6°C during the northern summer (Horel, 1982); this is so because of the geometry of the Pacific basin and the distribution of the continents in it. The prominent large-scale feature in the summertime temperature gradient fields is the negative meridional gradient over the northern subtropical Pacific, which is well correlated in the vertical; at 700 mb, its value ($\partial T'/ad\theta = -2$ K/1000 km) is about 70% of its surface value. During the northern winter, the temperature gradients are somewhat smaller, similarly correlated in the vertical till 700 mb, but with greater amplitude decay with height beyond 850 mb. During the FGGE summer, but not during FGGE winter, some features in the analyzed horizontal temperature gradients at even the 500 mb level remain correlated with the surface distribution; however, it is the convergence occurring below this level that largely determines the tropical precipitation. The high degree of correlation is compatible with the expected degree of mixing in the trade cumulus boundary layer. From Fig. 1, we see that this picture may not be totally appropriate over land or near coasts. Where the land is dry, there is no obvious reason to assume a trade cumulus boundary layer of the type discussed.

In this paper we take a highly simplified approach to the flow forced by surface temperature gradients in the trade cumulus boundary layer. We consider this layer to be topped by a surface (taken here to be 700 mb—roughly corresponding to the height of the trade inversion over the Pacific in summer). We eliminate all influences from above on the height of this surface; we also set all stresses at this upper surface to zero. Thus all motion in this lower layer will be due to the pressure gradients resulting from the SST distribution which we take to be mixed upward through this layer—allowing for some attenuation. The utility of this approach will be illustrated in sections 2 and 3.

Our objective here is to assess the potential importance of the "locally forced" lower tropospheric circulation in determining the net "near-surface" flow and convergence over the tropical oceans. In connection with the zonally averaged Hadley circulation, the ignored influence of flow above 700 mb is clearly significant, since the net angular momentum transport by the upper branch of the Hadley circulation can only be balanced by surface stresses which in turn require

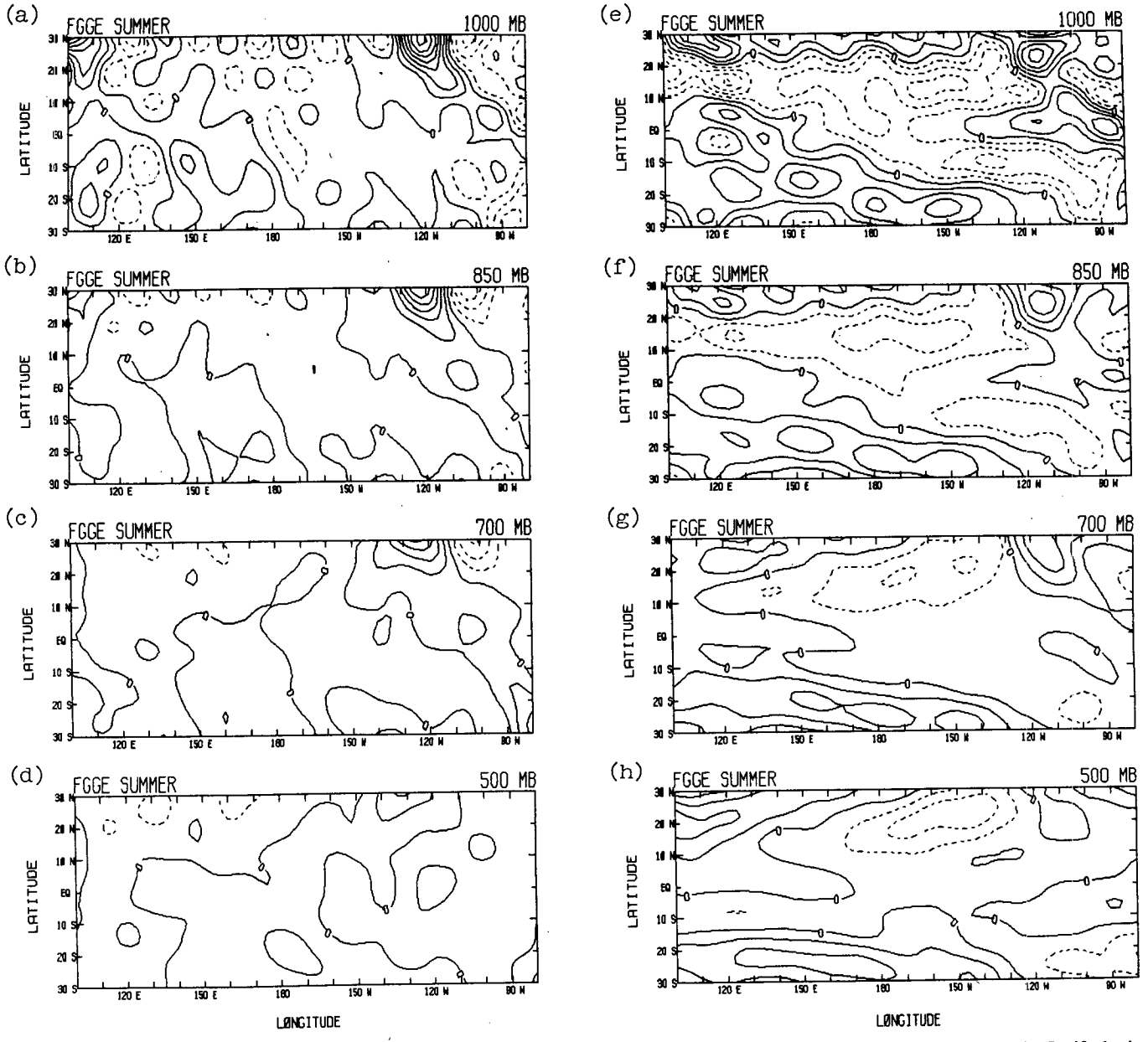


FIG. 1. The horizontal gradients in the ECMWF analyzed eddy virtual temperature field are shown at four pressure levels over the Pacific basin during the FGGE summer; zonal gradients in parts (a)–(d) and meridional gradients in parts (e)–(h). The contour interval is $10^{-6}$ K m$^{-1}$ (or 1 K/1000 km), negative values are contoured using dashed lines, and the first solid contour is the zero contour.

induced surface winds (Schneider, 1977; Held and Hou, 1980). No similar constraint appears to pertain to the eddy motions. Our results are consistent with this situation. The observed zonally averaged surface zonal winds differ significantly from those directly forced by surface temperature distributions, while the eddy components of the surface wind are frequently well simulated by those forced exclusively by surface tempertaure variations. However, even in the zonally averaged case, the low-level convergence appears to be largely due to the motions forced by the surface temperature distribution. This is consistent with the findings of Schneider (1977). The zonally averaged case is discussed in section 5. Using our simple model we calculate the pressure gradients, winds and convergence field in the trade cumulus boundary layer; these solutions are then compared with the analyzed monthly mean FGGE data over the Pacific. The extent to which we obtain agreement is taken to be indicative of the extent to which these fields within the boundary layer are determined by surface temperature distributions. As we shall see, the extent is substantial.

In section 2a, we give the details of the simplest version of our model (wherein the height of the 700 mb surface is held constant) and apply it to the zonally *asymmetric* flow. An examination of the lower tropospheric tropical flow, and in particular the convergence field, forced by the 1000 mb temperature field and computed using this model demonstrates the shortcoming of fixing the 700 mb height; this condition is relaxed in section 3a. The solutions obtained with the full model are compared with the corresponding FGGE flow for both the summer and winter seasons in section 3. The solutions obtained in section 3 are analyzed further in section 4 to identify the essential contributors to tropical momentum balance and convergence in the moist layer below 700 mb; the sensitivity of solutions to various parameters is also discussed in that section. The zonally symmetric model and model solutions forced by the meridional gradient of zonally averaged surface temperature during FGGE summer and winter are contained in section 5. Summary and conclusions follow in section 6.

## 2. Model development and solutions

### a. *Model development*

As shown in Fig. 1 and discussed in the Introduction, the zonally asymmetric temperature field in the trade cumulus boundary layer is quite similar to the surface (1000 mb) temperature distribution except for the amplitudes; over the tropical Pacific, the amplitudes of the prominent large-scale features decay in the vertical, typically falling to 70% of their surface value at 700 mb ($Z$ = 3000 m). A simple albeit approximate representation of the three-dimensional temperature structure in the tropical lower troposphere in terms of the surface temperature distribution is

$$T(\lambda, \theta, z) = \bar{T}_s - \alpha z + T'_s\left(1 - \frac{\gamma Z}{H_0}\right), \tag{1}$$

where the overbar denotes zonal mean and the prime the deviation from it. $\alpha$ = .003 K m$^{-1}$, $\gamma$ = 0.30, $H_0$ = 3000 m and $T_s(\lambda, \theta)$ is the given surface temperature distribution. The zonally averaged temperature is thus assumed to decay with height with a lapse rate $\alpha$ at all latitudes. Because we allow the eddy component of $T'$ to decrease with height, there must also be an eddy variation of static stability ($\gamma T'_S/H_0$). However, quantitatively this perturbation is very small. Indeed, allowing perturbation amplitudes to decrease some 30% between 1000 and 700 mb also proves unimportant (compared to other uncertainties including those in the analyzed data). Further, as we intend to model the flow only in the trade cumulus boundary layer, it is convenient to assume $\rho = \rho(T)$ alone, i.e., the boundary layer flow to be essentially incompressible. To first order, the density's dependence on temperature can then be expressed as

$$\rho = \rho_0[1 - n(T - T_0)], \tag{2a}$$

where

$$\rho_0 = \rho(T_0) = 1.225\,\text{kg m}^{-3}, \quad T_0 = 288\,\text{K},$$

$$n = -\left[\frac{1}{\rho}\frac{\partial \rho}{\partial T}\right]_{T_0} = 1/T_0,$$

so that

$$\rho = \rho_0[2 - nT]. \tag{2b}$$

From the knowledge of density and temperature fields, the three-dimensional pressure field can be constructed using the hydrostatic equation and a boundary condition or an integration constant; assuming the latter to be a specification of the geopotential height field $Z_T(\lambda, \theta)$ of an isobaric surface $p_T$, the pressure field, $p$, when $p > p_T$, is

$$p(\lambda, \theta, Z) = p_T + g\rho_0(2 - nT_s)(Z_T - Z) + \frac{g\rho_0 n}{2}\left(\alpha + \frac{\gamma T'_s}{H_0}\right)(Z_T^2 - Z^2), \tag{3}$$

where $T_s = \bar{T}_s + T'_s$.

For a simple dynamical description of the steady tropical flow, the curvature and advection terms in the zonal and meridional momentum equations can be neglected but the horizontal components of the vertical turbulent stress term must be retained because of our interest in the near-surface flow; the simplified equations are

$$-fv = \frac{1}{\rho a \cos\theta}\frac{\partial p}{\partial \lambda} + \frac{1}{\rho}\frac{\partial \tau_x}{\partial z} \tag{4}$$

$$fu = -\frac{1}{\rho a}\frac{\partial p}{\partial \theta} + \frac{1}{\rho}\frac{\partial \tau_y}{\partial z}, \tag{5}$$

where

| | |
|---|---|
| $\lambda$, $\theta$ | the longitude and latitude, respectively, |
| $a$ | (=6.371 × 10$^6$ m) the radius of the earth, |
| $f$ | ($2\Omega \sin\theta$) the variable Coriolis parameter, |
| $\Omega$ | (=7.272 × 10$^{-5}$ s$^{-1}$) the earth's angular velocity, |
| $u$, $v$ | the zonal and meridional components of velocity, respectively, |
| $\rho$ | [=$\rho(\lambda, \theta, z)$] the density, |
| $p$ | [=$p(\lambda, \theta, z)$] the pressure, and |
| $\tau_x$, $\tau_y$ | the zonal and meridional components respectively of the vertical turbulent stress. |

The pressure field and therefore the horizontal flow could be determined if $Z_T(\lambda, \theta)$ were known or simultaneously determined. A zero-order approximation is to set $Z_T(\lambda, \theta)$ to a constant; $Z_T = H_0$ = 3000 m ($p_T$ ~ 700 mb). We will show in section 2b that this zero-order approximation does in fact yield a reasonable eddy surface pressure field. However, to get reasonable solutions for the horizontal flow too, it is essential, as

we shall see later, that $Z_T$ be allowed to vary in response to low-level convergence.

When the expression for pressure [(3)] is inserted in the horizontal momentum equations, the mass-weighted vertical averaging of (4)–(5) in the layer extending from the surface to $Z_T$ ($=H_0$) yields

$$-fV = -\frac{g}{a\cos\theta}\left[-Q\frac{dT_s'}{d\lambda}\right] + \frac{\tau_{x|_{Z_T}} - \tau_{x|_0}}{\rho_0 Z_T} \tag{6a}$$

$$fU = -\frac{g}{a}\left[-Q\frac{dT_s'}{d\theta} - \frac{nZ_T}{2}\frac{d\bar{T}_s}{d\theta}\right] + \frac{\tau_{y|_{Z_T}} - \tau_{y|_0}}{\rho_0 Z_T} \tag{7a}$$

where

$$Q = \left(\frac{nZ_T}{2}\right)\left[1 - \frac{2\gamma Z_T}{3H_0}\right],$$

$$(U, V) = \left[\frac{1}{\rho_0 Z_T}\right]\int_0^{Z_T}(u, v)\rho dz \quad \text{with} \quad Z_T = H_0.$$

In line with ignoring the effects of circulation above $Z_T$, we set the turbulent stress at $Z = Z_T$ to zero. The need to balance Hadley transports of angular momentum with surface stresses invalidates this assumption for axially symmetric zonal flows (Schneider, 1977; Held and Hou, 1980). The eddy stress at the surface is expressed, as customary, in terms of drag coefficient, $C_d$, and the wind speed as

$$(\tau_x, \tau_y)| = -\rho_0 C_d (U^2 + V^2)^{1/2}(U, V).$$

of (6a)–(7a), when linearized about a state of rest, is

$$-fV' = -\frac{g}{a\cos\theta}\left[-\frac{nH_0}{2}\left(1 - \frac{2\gamma}{3}\right)\frac{\partial T_s'}{\partial\lambda}\right] - \epsilon U' \tag{6b}$$

$$fU' = -\frac{g}{a}\left[-\frac{nH_0}{2}\left(1 - \frac{2\gamma}{3}\right)\frac{\partial T_s'}{\partial\theta}\right] - \epsilon V', \tag{7b}$$

where $\epsilon = C_d|V|_c/H_0$ and $|V|_c$ is some constant typical wind speed in the trade cumulus boundary layer; all other symbols have been defined before. Most of the solutions are obtained used a value of $\epsilon = (2.5 \text{ days})^{-1}$, which for $H_0 = 3000$ m and $|V|_c = 8$ m s$^{-1}$ implies a $C_d$ equal to $1.736 \times 10^{-3}$. Such a value of the drag coefficient is consistent with that given, for example, in Wu (1980). The sensitivity of model solutions to the value of the Rayleigh drag, $\epsilon$, is discussed in section 4. Equations (6b) and (7b) are linear simultaneous algebraic equations in $U'$ and $V'$, and can therefore be solved independently at each grid point. When solving the above algebraic system, the smoothed forcing field $T_s$ is made available on a sufficiently fine grid: $\Delta\lambda = 3°$, $\Delta\theta = 1°$. The model solutions are described in subsection 2b.

Because of the considerable humidity in the trade cumulus boundary layer, all model calculations, unless stated otherwise, are done using the virtual surface temperature ($T_{vs}$). The $T_{vs}$ is related to $T_s$ as follows:

$$T_{vs}(\lambda, \theta) = T_s(\lambda, \theta)\left(1 + \frac{0.61q}{1-q}\right)$$

where $q$, the specific humidity, is expressed in units of (kg of water)/(kg of moist air). The gradients in $T_{vs}$ are larger than those in $T_s$ by 15% to 20%, and so the difference in model solutions due to the use of $T_{vs}$ rather than $T_s$ is simply in the amplitudes.

And finally, all the FGGE fields used in this study either as inputs to the model (e.g., $T_{vs}$) or else for the purposes of comparison with the model solutions are first smoothed by fitting spherical harmonics to the ECMWF's analyzed grid point fields ($\Delta\lambda = 5°$, $\Delta\theta = 4°$) and then reconstructing the grid point fields from the spectral amplitudes using a rhomboidal truncation at wavenumber 15 (i.e., R15).

### b. *Model solutions*

The 1000 mb summertime (FGGE) virtual temperature field used to force the model is shown over the tropical Pacific in Fig. 2a. The tropical western Pacific is, as expected, warmer than the eastern Pacific by about 6°C. In the central tropical Pacific, the meridional gra-

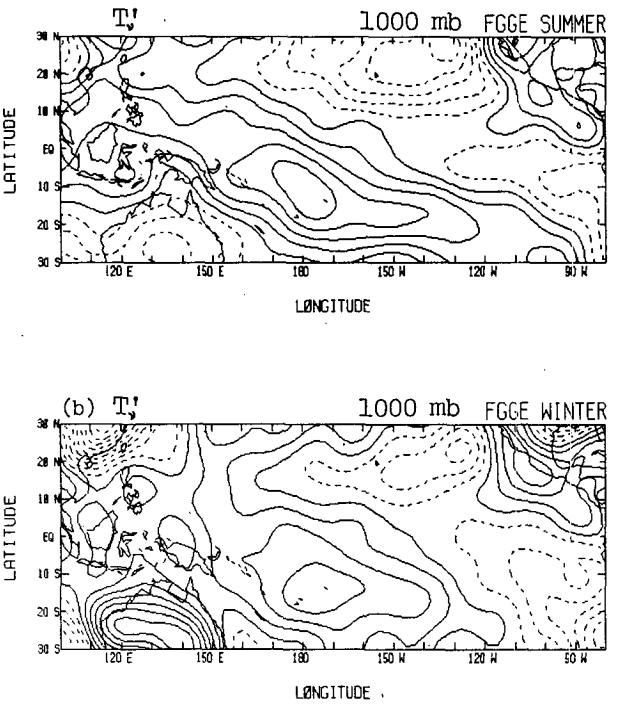


FIG. 2. The 1000 mb eddy virtual temperature fields are obtained from a smoothed version of the ECMWF FGGE analyses. The summertime field is shown in (a) and the wintertime field in (b) using a contour interval of 1 K; the contouring convention is as in Fig. 1.

dients are considerably larger than the zonal gradients as was also seen in Fig. 1. The linearized eddy sea level pressure field shown in Fig. 3a is almost identical in phase with the 1000 mb eddy virtual temperature field; thus, our parameterization of the vertical structure of the tropical temperature field [Eq. (1)] together with the assumption of pressure gradients vanishing at the top of our boundary layer (taken to be at 3 km) results in a "surface low" over the warm tropical SSTs and a relative "surface high" over the cold tropical SSTs. The expression for the linearized eddy sea-level pressure, obtained from (3) with $Z_T = 3000$ m, is

$$p'_{SL}(\lambda,\theta) = g\rho_0 n H_0\left(\frac{\gamma}{2}-1\right)T'_s.$$

That the above expression for eddy sea-level pressure provides a fairly reasonable description of the corresponding observed field is apparent from a comparison of Figs. 3a and 3b; the latter is the eddy sea-level pressure during the FGGE summer as analyzed by the ECMWF. The correspondence between the two fields over the tropical and subtropical oceans ($|\theta| < 20°$) is considerable and indeed surprising given the simplicity of our formulation. There are subtle differences between the two fields in the vicinity of the equator which although minor in terms of amplitude (<1 mb) are of great consequence for the equatorial flow; this is discussed at length towards the end of this section and also in the subsequent section.

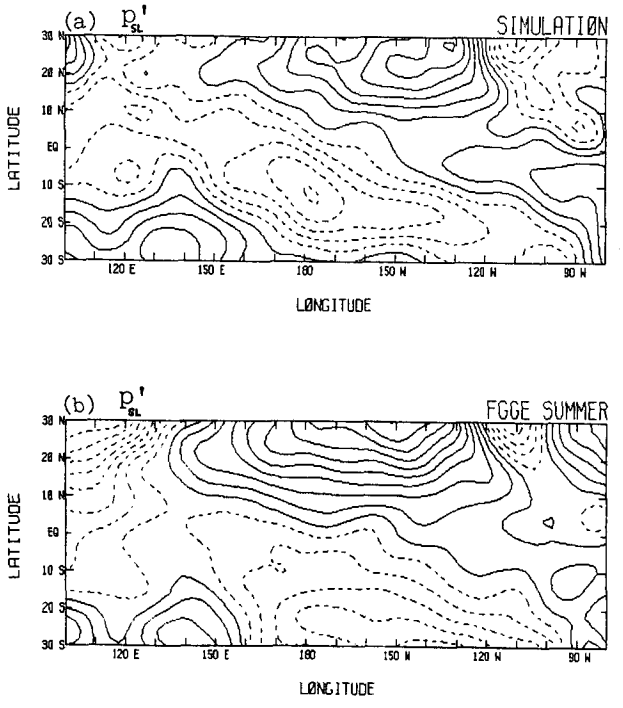


FIG. 3. (a) The summertime eddy sea-level pressure computed using (8a); (b) the corresponding observed field, obtained from the ECMWF analyses for the FGGE summer. The contour interval is 1 mb, and the contouring convention is as in Fig. 1.

The low-level (mass weighted vertical average over the lowest 3 km) tropical flow forced by this eddy virtual temperature field is shown in Fig. 4—the eddy zonal and meridional velocity fields in parts (a) and (b) respectively, and the convergence field in part (c). It is immediately clear that the simulation of winds and—especially—divergence near the equator is awful. Notice in particular the large amplitudes and the rapid phase variations (or the large meridional shears) of the eddy fields near the equator and the date line: the zonal wind has an easterly maximum of 21 m $s^{-1}$ whereas the meridional wind there is from the north and about 27 m $s^{-1}$. The eddy convergence along the equator is at least as large as $(5 \times 10^{-5})$ $s^{-1}$ which is more than 10 times the observed value of the low-level tropical convergence. As expected in such situations, the solutions are strongly dependent on the model's meridional resolution. As it turns out, the use of a coarser latitudinal grid ($\Delta\theta = 4°$) results in a solution that on the face of it appears realistic, but this is hardly an acceptable approach.

Using a nonlinear surface stress formulation and increasing $\epsilon$ to (1 day)$^{-1}$ "improved" the wind simulation somewhat, but tropical convergence remained enormous.

It is interesting to note that even though our approach plausibly simulates pressure distributions, it fails to simulate winds in the lower troposphere (trade cumulus layer). This is indicative of the sensitivity of near-equatorial winds to almost imperceptible variations in the equatorial pressure field. In nature, the winds would redistribute air slightly so as to correct the pressure, but in the present oversimplified version of our model this does not happen. Horizontal convergence would normally act to effect such a redistribution, but in the present model which has a rigid flat top it is assumed that the convergence is instantaneously taken up by the cumulonimbus mass flux $M_c$. According to Lindzen's (1981) cumulus parameterization

$$M_c = -\int_0^{Z_T} \nabla\cdot\rho\vec{\mathbf{V}}dz + E/q, \qquad (8)$$

where $E$ is the evaporation measured in units of kg $m^{-2}$/sec. While the above is known to be a good approximation in the conditionally unstable tropics, the take-up of horizontal convergence by $M_c$ does not occur instantaneously in nature. When a finite adjustment time is allowed, a small fraction of mass converged per unit area acts to redistribute air within the trade cumulus boundary layer so as to modify the pressure gradients slightly (but as we shall see, with immense consequences for calculated convergence). Within the present model, such air redistribution is most easily handled by allowing perturbations, $h'$, in the height of

our boundary layer. However, once the steady state is realized, all the convergent mass exits the trade cumulus layer. In nature, this adjustment time is determined essentially, we believe, by the time deep cumulus clouds take to develop [O(1 h)]. The consequent development of a "back pressure," as we shall see in the following subsection, results in a vertically averaged steady state convergence that is much smaller than that obtained by excluding the same effect.

### 3. Eddy solutions obtained with the "back-pressure" field included

#### *a. Problem formulation*

In this section, the simple linear model is modified to incorporate the effects of a "back-pressure" field. In our simple one-layer model the only way to do this is by allowing the height of the boundary layer (considered to be an isobaric surface with a pressure $p_T = 700$ mb) to be variable and therefore responsive to convergence of mass during the transient establishment of the steady-state low-level convergence field. The "back-pressure" field, a negative feedback of sorts, is generated due to the modulation of geopotential height of the isobaric surface $p_T$. The top of this layer is therefore expressed as

$$Z_T(\lambda,\theta) = H_0 + \bar{h}(\theta) + h'(\lambda,\theta) \tag{9a}$$

where

$H_0$ is the spatially constant part which is set equal to 3000 m,

$\bar{h}(\theta)$ is the latitudinally dependent part which, in the absence of any zonally symmetric flow, is identically zero; otherwise $|\bar{h}/H_0|$ is expected and assumed to be $\ll 1$, and

$h'(\lambda, \theta)$ is the horizontally inhomogeneous part which too is expected and assumed to be much smaller than $H_0$, i.e., $|h'/H_0| \ll 1$.

The sea level pressure, like pressure at any other height in the boundary layer, now has a contribution from the yet undetermined height variations as well; the linearized eddy sea-level pressure is determined as

$$p'_{SL} = g\rho_0 nH_0\left(\frac{\gamma}{2} - 1\right)T'_s + g\rho_0(2 - n\bar{T}_s + n\alpha H_0)h'. \tag{9b}$$

As $h'$ is not known a priori, the vertically averaged pressure gradients are not fully determined, and therefore neither are $U'$ and $V'$. To solve for $h'$ simultaneously with $U'$ and $V'$, one must, in addition to the momentum equations, consider the vertically averaged (through the boundary layer) continuity equation, too, which relates $h'$ and horizontal convergence through a time scale, $\tau_c$.

It is shown in appendix A that when the balance given by (8) is associated with an adjustment time $\tau_c$, then $h'$ is given by

$$h' = \tau_c \frac{H_0}{a\cos\theta}\left[\frac{\partial U'}{\partial\lambda} + \frac{\partial(V'\cos\theta)}{\partial\theta}\right]. \tag{10}$$

As noted in appendix A, $h'$ is proportional to $M'_c$. $\tau_c$ is the time it takes $M'_c$ to adjust to the low-level convergence, and during this adjustment time, the convergence can redistribute mass and produce a "back pressure" by way of the variation in $Z_T$ given by (10).

The vertical averages of (4) and (5), where $p$ is given as before by (3) but now with $Z_T = H_0 + \bar{h} + h'$, are linearized about a resting basic state[1] (i.e., $\bar{U} = \bar{V} = 0.0$); the resulting eddy momentum equations are

$$-fV' = -\frac{g}{a\cos\theta}\left[(2 - n\bar{T}_S + n\alpha H_0)\frac{\partial h'}{\partial\lambda} - \frac{nH_0}{2}\left(1 - \frac{2\gamma}{3}\right)\frac{\partial T'_s}{\partial\lambda}\right] - \epsilon U' \tag{6c}$$

$$fV' = -\frac{g}{a}\left[(2 - n\bar{T}_S + n\alpha H_0)\frac{\partial h'}{\partial\theta} - \frac{nH_0}{2}\left(1 - \frac{2\gamma}{3}\right)\frac{\partial T'_s}{\partial\theta} - \frac{nh'}{2}\frac{\partial\bar{T}_s}{\partial\theta}\right] - \epsilon V'. \tag{7c}$$

In this simple one-layer model, the dependence of the steady-state horizontal convergence ($h'/\tau_c$) on $\tau_c$ is not straightforward as $h'$ is itself sensitive to the value of $\tau_c$. This subtle dependence is best understood by thinking about the transient adjustment phase during which undulations in the height ($h'$) are allowed to develop so that horizontal convergence and the "back-pressure" effect, each expressed in terms of $h'$ and dependent on each other in this one-layer model, become mutually adjusted in the steady state. The numerical procedure used to obtain the steady-state solutions is described in appendix B.

When the back-pressure effect is small, the convergence is excessive (as seen in Fig. 4c which is obtained without any back-pressure effect), and so is the product of $\tau_c^{-1}$ and $h'$; the large product must, however, result from a small $\tau_c$ and not a large $h'$. This is because if $h'$ were large instead of $\tau_c^{-1}$ the pressure gradients forced by the surface temperature field would be neutralized by those forced by undulations in the layer height. The new model [(6c), (7c) and (10)] should thus be able to replicate the old model [(6b) and (7b)] results when $\tau_c$ is very small; this is to be expected as a small value of $\tau_c$ corresponds to an almost instantaneous relaxation that is accomplished by the quick exodus of approximately all the converged mass and this leaves little time for the development of a significant back-pressure field.

[1] To be strictly consistent with the assumption of the absence of any zonally symmetric forcing or flow, one must take $\bar{T}_s$ to be independent of latitude in (6c) and (7c). Eddy solutions obtained in this manner however differ negligibly (<1%) from those obtained using (6c) and (7c).

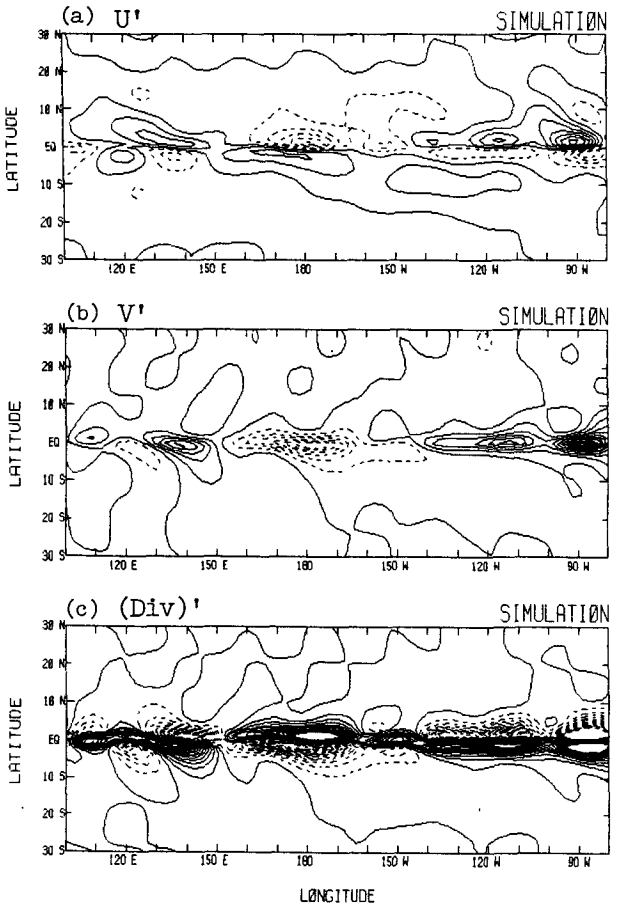


FIG. 4. The low-level summertime flow over the Pacific obtained from the simple linear model which has a uniformly deep trade cumulus layer ($H_0$ = 3000 m) and with $\epsilon$ = (2.5 days)$^{-1}$; $U'$ and $V'$ are shown in (a) and (b) respectively using a contour interval of 4 m s$^{-1}$, whereas the eddy divergence is shown in (c) using an interval of 4 $\times 10^{-6}$ s$^{-1}$. Contouring convention as before, e.g., convergent regions are indicated by dashed contours.

In such a case, $h'$ will therefore be negligible though nonzero. For the same value of the Rayleigh friction coefficient, $\epsilon$ = (2.5 days)$^{-1}$, we were able to essentially reproduce the old linear model results using the new model with $\tau_c$ = 30 sec.

When the back-pressure effect or the negative feedback is very large, the convergence is small and results mostly from the largeness of $\tau_c$ and not from the smallness of $h'$; in such a situation, $h'$ will, in fact, be quite large and result in an almost complete neutralization of pressure gradients that are forced by the surface temperature gradients. The new model, with $\tau_c$ = 3 h, therefore yields solutions that are characterized by extremely weak tropical flow (<1 m s$^{-1}$ everywhere) and convergence (<$10^{-6}$ s$^{-1}$). Values of $\tau_c$ between 30 sec and 3 h yield solutions that differ only in amplitude and not in phase; the ones obtained using $\tau_c$ = 30 min appear to provide the best description of the low-level tropical flow observed during the FGGE summer. This is, indeed, on the order of the time taken by the cumulonimbus mass flux to adjust to the horizontal convergence.

It is worth noting that our modified model is analogous to that of Gill (1980) although he put forward his model to describe the response of the entire tropical troposphere to cumulus heating. As such, his assumption of a lid and a frictionally balanced momentum budget seems unjustifiable. The present model of the surface layer leads to the same equations used by Gill (1980). However, it involves both a significant reinterpretation of various features of Gill's model as well as a relatively concrete and objective basis for assigning the values of various parameters. These relations are summarized in Table 1.

Our solutions, obtained for both the FGGE summer and winter seasons using $\tau_c$ = 30 min, are compared with the corresponding ECMWF analyzed FGGE fields in the following subsection.

### *b. Model solutions for the FGGE summer and winter*

The summer and winter mean (FGGE year) 1000 mb eddy virtual temperature fields used to force the eddy dynamical model [(6c), (7c) and (10)] are shown in Figs. 2a and 2b, respectively. Immediately apparent is the considerable similarity between the two analyzed fields over much of the tropical Pacific Ocean. As the annual cycle in sea surface temperature is nearly homogeneous in phase and amplitude in the northern subtropical Pacific (Horel, 1982), the zonal temperature contrast (e.g., between longitudes 150°E and 130°W) does not depend much on seasons.[2] The amplitude of the annual SST cycle in the tropical south Pacific increases eastward with a phase that is nearly constant in longitude but such as to result in maximum SSTs in mid-March; the zonal contrast in SSTs there is therefore also rather similar during the winter and summer seasons.

The model solutions obtained using $\tau_c$ = 30 min and the summertime (FGGE) eddy virtual temperature are shown in Fig. 5: eddy zonal and meridional velocities in m s$^{-1}$ in parts (a) and (b), eddy divergence in units of (sec)$^{-1}$ in (c) and eddy sea-level pressure in mb in (d). The corresponding lower tropospheric averages of the analyzed FGGE fields, obtained by taking a quarter of the 1000 and 700 mb values and half of the 850 mb value, are also displayed in Figs. 5e–h. The first thing to notice is that the equator is no longer a problematic region: the modification of near-equatorial pressure field by the back-pressure effect has virtually eliminated most of the small-scale latitudinal structure present at the equator in solutions shown in Fig. 4

[2] In this region, the eddy amplitudes too would be similar in the two seasons if the eddy field was computed relative to the zonally averaged temperature in just the tropical Pacific basin and not relative to the zonal average computed using all the longitudes.

TABLE 1. Counterparts between Gill's (1980) model and the present model.

| Gill (1980) | Present model |
|---|---|
| Artificial lid at tropopause | Trade inversion, $Z_T$ |
| Thermal relaxation time | Cumulonimbus setup time |
| Artificial tropospheric friction | Surface drag |
| Artificial internal mode | Relatively mixed layer below $Z_T$ |
| Forcing nominally due to cumulus heating | Forcing calculably due to SST distribution |

which are contoured using intervals that are four times as large for horizontal velocities and ten times as large for the convergence in comparison with those used in Fig. 5. It must also be noticed that the improvements in the modeled tropical flow and convergence near the equator result from rather modest modifications (<1 mb) to the equatorial pressure field as is evident from a comparison of the modeled sea-level pressure fields (Fig. 3a and Fig. 5d), which underscores our earlier assertion that the near-equatorial flow is quite sensitive to even minute changes in the tropical pressure field.

Over the tropical Pacific, the model solutions compare favorably with the corresponding ECMWF analyzed FGGE fields: the zonal velocity field has almost the right amplitude and phase, the meridional velocity is now much smaller than in Fig. 4 and in line with FGGE field shown in Fig. 5f, and above all, the modeled tropical convergence now has reasonable amplitudes and good phase and amplitude correspondence with the analyzed FGGE convergence shown in Fig. 5g, e.g., within 20° of the equator, the south Pacific convergence zone (SPCZ) is simulated rather well. To be sure, there are differences between the two, e.g., near the equator and date line, the circulation features including the convergent zone are placed northward in the model solutions in comparison with the location of the same features in the FGGE fields; this difference is most apparent in the eddy sea-level pressure fields shown in Figs. 5d and 5h. Although our solutions show a certain degree of spatial coincidence between maxima in horizontal convergence (and hence precipitation) and maxima in SST, it is clear from the physics of our model that such coincidence is hardly essential.

The discrepancies between the model solutions and the analyzed FGGE fields are larger and often considerable over the continental landmasses irrespective of whether they are in the tropics or extratropics, e.g., over Australia, Central America and portions of the East Asian landmass included in the display–domain of the figures (see Fig. 2). Excluding these regions and other minor differences, the model solutions are by and large good within 20° of latitude of the equator. Better solutions may, for instance, be obtainable for different choices of $\epsilon$ and $H_0$. However, our intention was not to simulate precisely the analyzed FGGE fields, which are themselves uncertain representations, but to simply ascertain the importance of sea surface temperature gradients in determining the near-surface tropical flow. It is evident from our calculations that the contributions to the low-level flow generated directly by spatial variations in SST are as large as the observed flow itself and similarly distributed. Our calculations do not assess the influence of flows above 3 km on the low-level pressure gradients.

Our model depends on buoyant convection significantly mixing the lower troposphere (below about 3 km). Over tropical oceans this convection is forced primarily by evaporation from the surface. Presumably such forcing is also present over wet land. However, over dry land the nature of the boundary layer is likely to be more complicated and generally different from what has been assumed in this paper.

During FGGE winter, the horizontal temperature gradients in the lower troposphere are again correlated with the surface distribution over the tropical Pacific but the correlations weaken more rapidly in the vertical during winter; this could, for instance, be suggestive of the fact that the trade cumulus layer is shallower during winter or at least during FGGE winter. There is also some indication in the analyzed wintertime FGGE data that the pressure field within the trade cumulus layer has a component that is associated with atmospheric motions aloft. We nonetheless use the same dynamical model with the same parameters (notably $H_0$ = 3000 m, $\gamma$ = 0.30) to solve for the wintertime flow which is compared with the analyzed FGGE observations in Fig. 6; the format of Fig. 6 is identical to that of Fig. 5. The correspondence between model solutions and the analyzed FGGE fields over the tropical Pacific is no longer as good as during summertime: the prominent circulation features in the FGGE eddy zonal velocity field are, to an extent, present in model solutions but with weaker amplitudes and incorrect phases. The model solution captures the convergence occurring east of the Australian continent (SPCZ) but shows no evidence of an ITCZ in the eastern tropical Pacific; the latter is, perhaps, the most serious and noticeable discrepancy between Figs. 6c and 6g in the tropical Pacific. It is worth noting that a comparison of the two eddy sea-level pressure fields (Figs. 6d and 6h) alone would not have foretold the extent of differences in tropical circulation noted above; the latter may, indeed, be due to the aforementioned inadequacies in the way we have modeled the wintertime response to surface temperature forcing rather than to the forcing from above (which we have omitted).

## 4. Analysis of solutions

In this section, we analyze the "summertime" model solutions further to answer some related questions:

(i) Is the low-level tropical flow in the above described solutions forced by the zonal or the meridional gradients of SSTs or both?

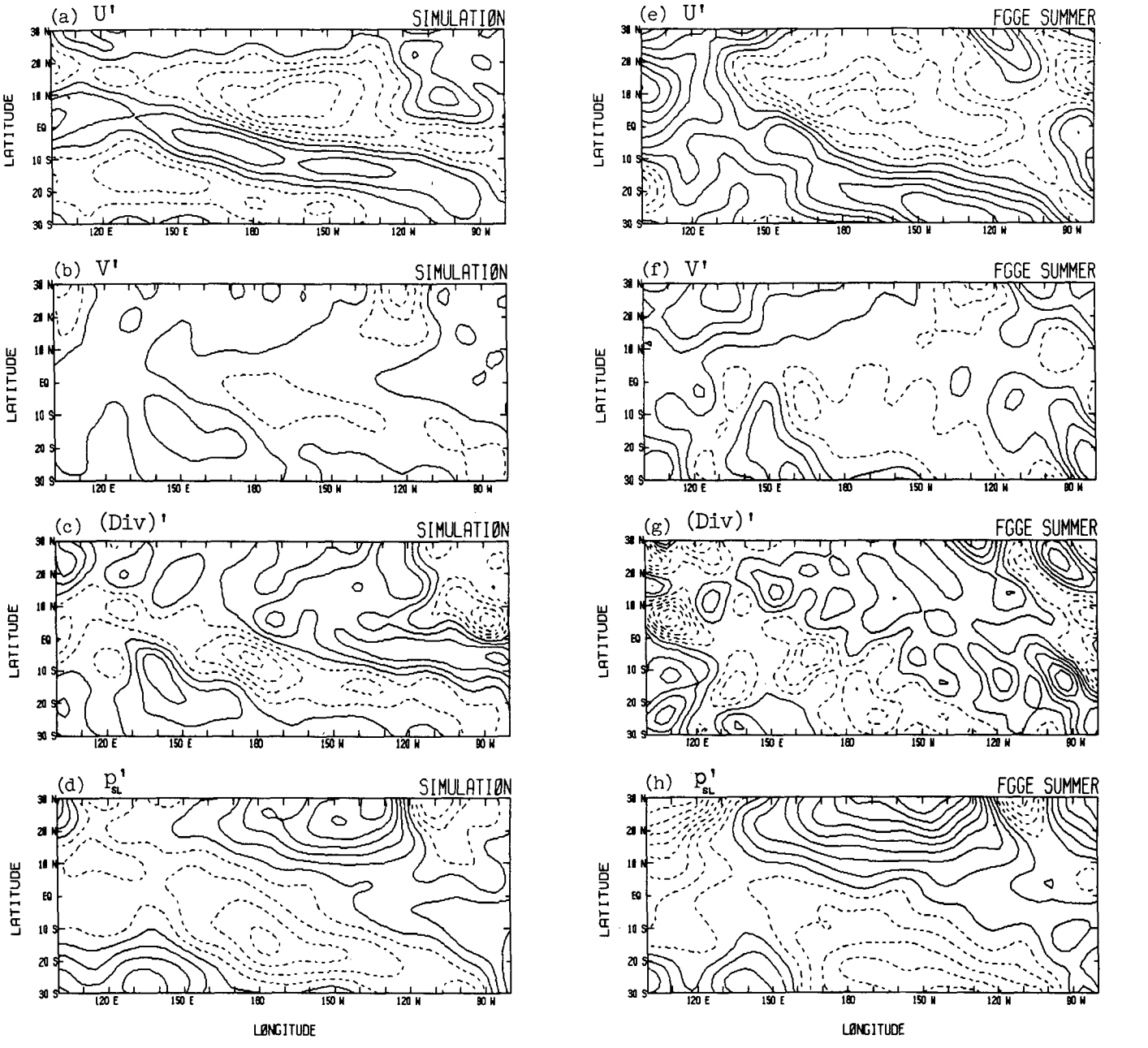


FIG. 5. The low-level summertime flow over the Pacific obtained from the linear model in which the boundary layer height is allowed to adjust to the horizontal convergence; $\epsilon = (2.5 \text{ days})^{-1}$, $\tau_c = 30$ min, $H_0 = 3000$ m. The model solutions are shown in the left panel whereas the corresponding fields from the ECMWF analysis are shown in the right panel. The contour interval is as follows: $U'$ and $V' = 1$ m s$^{-1}$, div $= 4 \times 10^{-7}$ s$^{-1}$, and $p'_{SL} = 1$ mb; negative values are contoured using dashed lines, and the first solid contour is the zero contour.

(ii) What is the essential horizontal momentum balance in the above solutions?

(iii) How important is the contribution of "beta convergence" (due to latitudinal variation of the Coriolis parameter) to the total convergence over tropical oceans?

(iv) How sensitive are the model solutions to the value of $\tau_c$?

As meridional gradients of SST are larger than zonal gradients over the tropical Pacific (Figs. 1a and 1e) by about a factor of 2, one expects the former to be the primary forcing in our model. This is ascertained by recomputing the summertime solution once with the zonal SST gradients set equal to zero, i.e., $dT'_s/d\lambda$ in (6c) to zero, and then with only the eddy meridional SST gradients set equal to zero; the eddy convergences

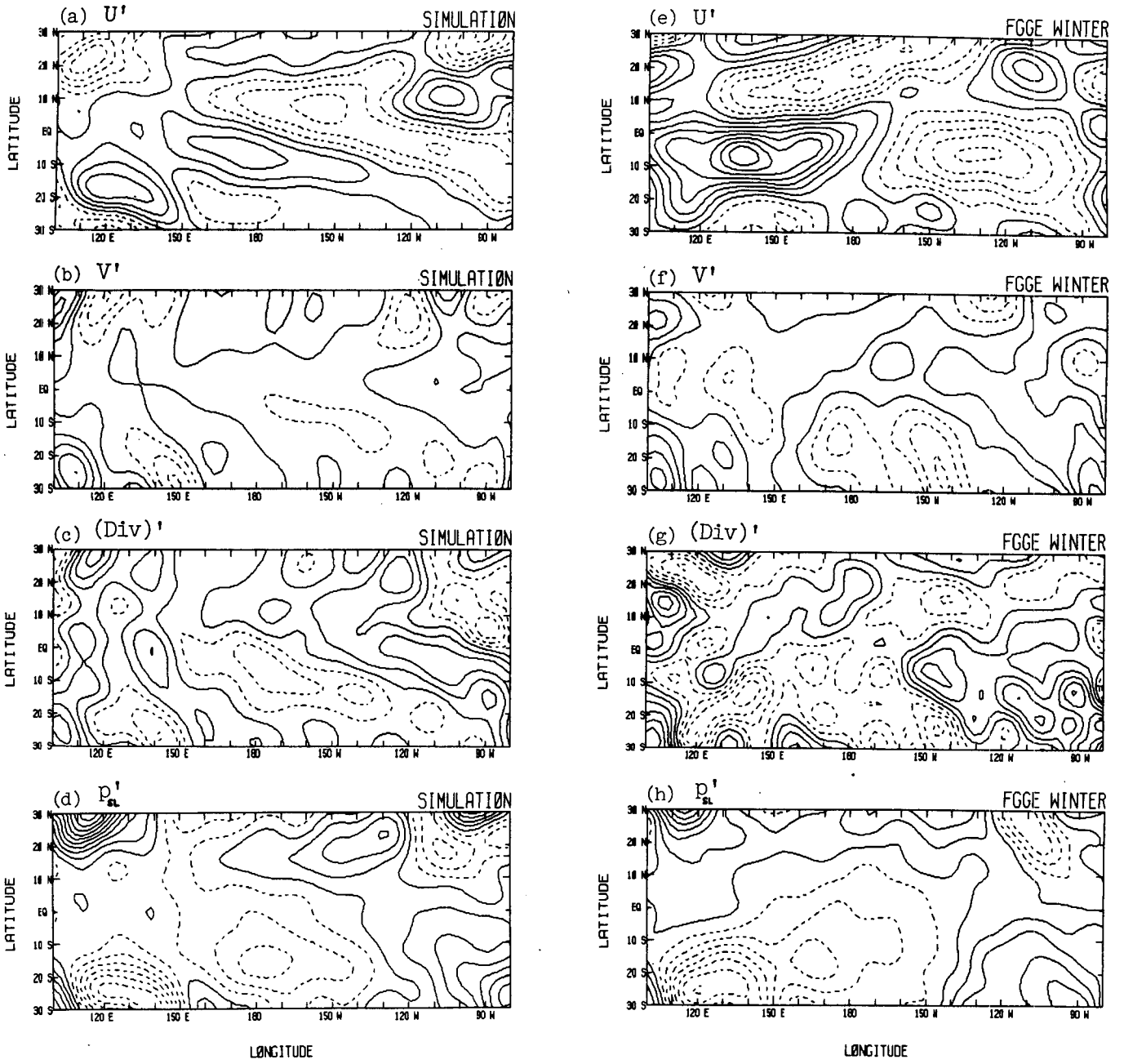


FIG. 6. As in Fig. 5 except for the FGGE winter.

thus obtained are shown in Figs. 7a and 7b, respectively. The first thing to notice is that the convergence forced by zonal gradients in SST is considerable and even comparable to that forced by the meridional SST gradients. A comparison of Figs. 7a and 7b with Fig. 5c shows that a large fraction of the total convergence in the eastern tropical Pacific is forced by the meridional gradients in SST whereas in the central and western tropical Pacific, it is the zonal gradients of SST that are the major contributors. In the subtropics of both hemispheres, there is considerable cancellation between the two forced responses (Figs. 7a and 7b). The zonal gradients in SST, although smaller than the meridional gradients, can force a response comparable to that forced by the latter, only because the convergence is allowed to create a back pressure; such feedback produces height gradients which attenuate the effects of SST gradients in proportion to the latters' strength. Without this feedback, the individual responses are likely to be commensurate with the magnitude of the

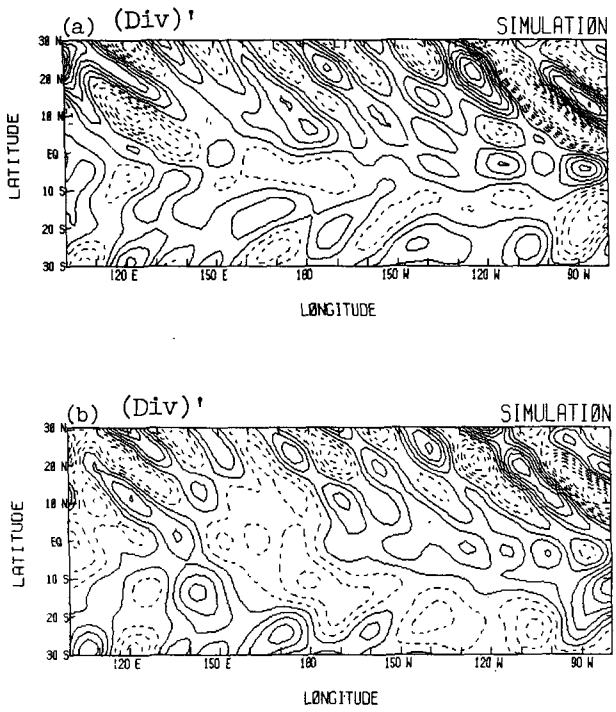


FIG. 7. The modeled summertime eddy divergence shown in Fig. 7c is split into two parts; the component forced by meridional gradients of the eddy SST field is shown in part (a), whereas that forced by the zonal gradients of SST is shown in (b). Contour interval and convention is as in Fig. 6c.

corresponding forcing functions. The above described decomposition of the summertime solution indicates that longitudinal variations in the low-level flow and convergence over the tropical Pacific (i.e., the Walker circulation in the lower troposphere) are forced not only by zonal gradients of SST, as commonly believed, but also by the zonal variations in the meridional SST gradient field.

The momentum balance in the model's tropics is essentially geostrophic in nature to within a few degrees of the equator; the value of the Rayleigh friction coefficient ($\epsilon$) used in all calculations described in section 3, is (2.5 days)$^{-1}$. This is also the value of $f$ at $\sim 1.82°$, and so the above result is not surprising. We demonstrate the character of the model's momentum balance by recomputing the full solution with an $\epsilon$ that is more than twice the old value, i.e., with $\epsilon$ = (1.0 day)$^{-1}$ which is also the value of $f$ at $\sim 4.6°$. The new horizontal flow and convergence field are shown in Fig. 8: the eddy meridional velocity and convergence (and therefore $h'$) are generally similar to those obtained with $\epsilon$ = (2.5 days)$^{-1}$ (Figs. 5b and 5c), even near the equator. The eddy horizontal velocity however shows more sensitivity to $\epsilon$ in the near-equatorial region as evident from a 50% reduction in amplitude of tropical westerlies in Fig. 8a; away from the equator, even this field is relatively insensitive to $\epsilon$. Because of the potential for feedback on pressure gradients in our model, it is in general difficult to predict the sensitivity or insensitivity of various dynamical quantities of $\epsilon$. If momentum balance in the subtropics was frictional instead of geostrophic, a change in $\epsilon$ by a factor of 2 would have resulted in a similar order change in the horizontal velocity amplitudes there; that is, however, not observed in the model solutions.

Before answering question (iii), we clarify what precisely we mean by "beta convergence." Using symbols P and R for the net zonal and meridional pressure gradient force in (6c) and (7c), one can write the latter compactly as

$$-fV' = -P - \epsilon U' \tag{11a}$$

$$fU' = -R - \epsilon V', \tag{11b}$$

where $P$ and $R$ depend on the known $T_S$ and on $h'$ which is a priori unknown. The divergence, diagnosed in terms of $P$, $R$, $\epsilon$ and $f$ alone, is

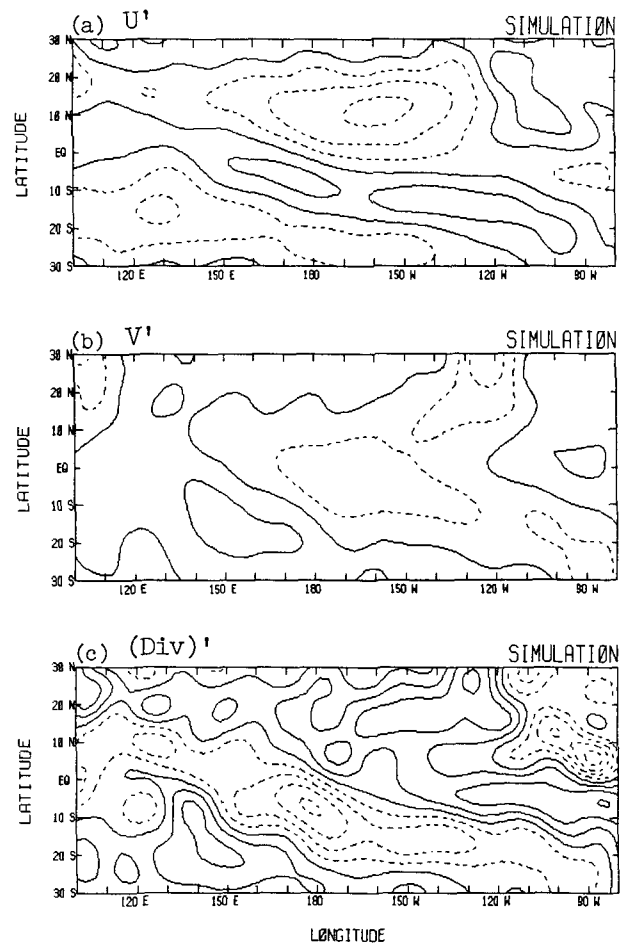


FIG. 8. The sensitivity of the summertime solutions to parameter $\epsilon$. Figures as in Figs. 6a–c except that the Rayleigh friction coefficient $\epsilon$ is now (1 day)$^{-1}$.

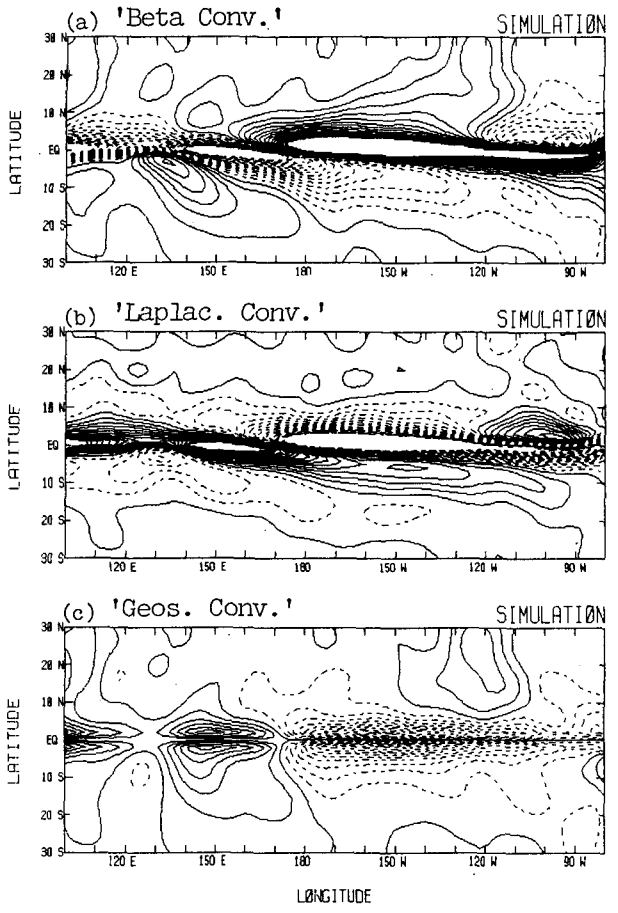


FIG. 9. The modeled summertime eddy divergence (Fig. 7c) is split up to identify the importance of various contributing terms: (a) beta convergence, (b) Laplacian convergence, and (c) geostrophic convergence. For a definition of these terms see section 4; note that geostrophic convergence, as defined, is a part of beta convergence. Contours as in Fig. 7c.

$$\frac{1}{a\cos\theta}\left[\frac{\partial U'}{\partial\lambda}+\frac{\partial(V'\cos\theta)}{\partial\theta}\right]$$

$$=\beta\frac{[(\epsilon^2-f^2)P+2f\epsilon R]}{(\epsilon^2+f^2)^2}+\left\{-\epsilon\left[\frac{\partial P}{\partial\lambda}+\frac{\partial R\cos\theta}{\partial\theta}\right]\right.$$

$$\left.+f\left[\frac{\partial P\cos\theta}{\partial\theta}-\frac{\partial R}{\partial\lambda}\right]\right\}\Big/(\epsilon^2+f^2)a\cos\theta \quad (11c)$$

where $\beta=(2\Omega\cos\theta)/a$. The first term on the right-hand side of (11c) exists only because the Coriolis parameter is a function of latitude. We refer to this contribution as "beta convergence." Note that beta convergence is different from geostrophic convergence $[=-\beta f^2P/(\epsilon^2+f^2)^2]$ in that it has contributions from the frictionally controlled component of the flow too. The second term on the rhs is referred to in the subsequent discussion as the "Laplacian term" because it is essentially determined by the first term in its numerator which is nothing but the Laplacian of the net pressure field multiplied by $[-\epsilon(\epsilon^2+f^2)]$; the second term in the numerator is nearly zero as it is approximately the curl of a gradient field.

In the subtropics, the net convergence in Fig. 5c is the sum of comparably sized but oppositely signed contributions of beta convergence and the Laplacian term; the decomposition of the eddy convergence field is shown in Fig. 9. In the near-equatorial region, the convergence has immense contributions from both beta convergence and Laplacian terms which are again diagnosed to be of opposite sign; their sum is, however, modest and precisely that shown in Fig. 5c. That the beta convergence is as large as shown in Fig. 9a and that its sign determines the sign of the net convergence over extended stretches of the tropical and subtropical Pacific seemed surprising. In a simple-minded description of the tropical flow, the momentum balance could be taken, for example, to be between just the friction and the pressure gradient terms, and in such case, the tropical convergence is determined essentially by the Laplacian of the net pressure field. The analysis of our model solutions indicates that the Laplacian contribution is of the right sign only in some subtropical regions, and that even there as elsewhere, it is severely modulated by the beta contribution. Thus, the simple-minded description of tropical dynamics mentioned above is inaccurate. The contribution of the geostrophic convergence is shown in Fig. 9c; in the tropics, its amplitudes are 2 to 3 times those of the net convergence and its phase is also not related to the latter's in any systematic manner.

The anticipated sensitivity of model solutions to the value of $\tau_c$ was discussed at length when describing the formulation of the model in section 3a. Here we display the observed sensitivity of solutions to $\tau_c$ graphically. In Fig. 10, we show the eddy horizontal velocity, geopotential height and the convergence fields for two other values of $\tau_c$: parts (a)–(c) describe the solutions when $\tau_c$ = 10 min whereas parts (e)–(f) describe those obtained using $\tau_c$ = 3 h. It is clear that when $\tau_c$ is decreased, the geopotential height amplitudes diminish whereas the convergence and horizontal flow become stronger: when $\tau_c$ is decreased even further, e.g., say to 1 min, these fields start to resemble those obtained from the oversimplified model in section 2. At $\tau_c$ is decreased, the horizontal convergence has even less time to generate a back pressure with the result that there is then little, if any, feedback; the steady state horizontal convergence therefore differs little from what it is in the complete absence of any feedback (section 2).

The amplitude of the vertically averaged tropical flow also depends on the depth of our boundary layer, $H_0$; however the dependence on $H_0$ is weaker than the solutions' sensitivity to other model parameters. When the boundary layer depth is decreased (to say 2 km) without altering the vertical structure of the eddy temperature field [i.e., $H_0$ in (1) is kept fixed], the linearized vertically averaged pressure gradients resulting from the SST distribution decrease (by ~25%) while the

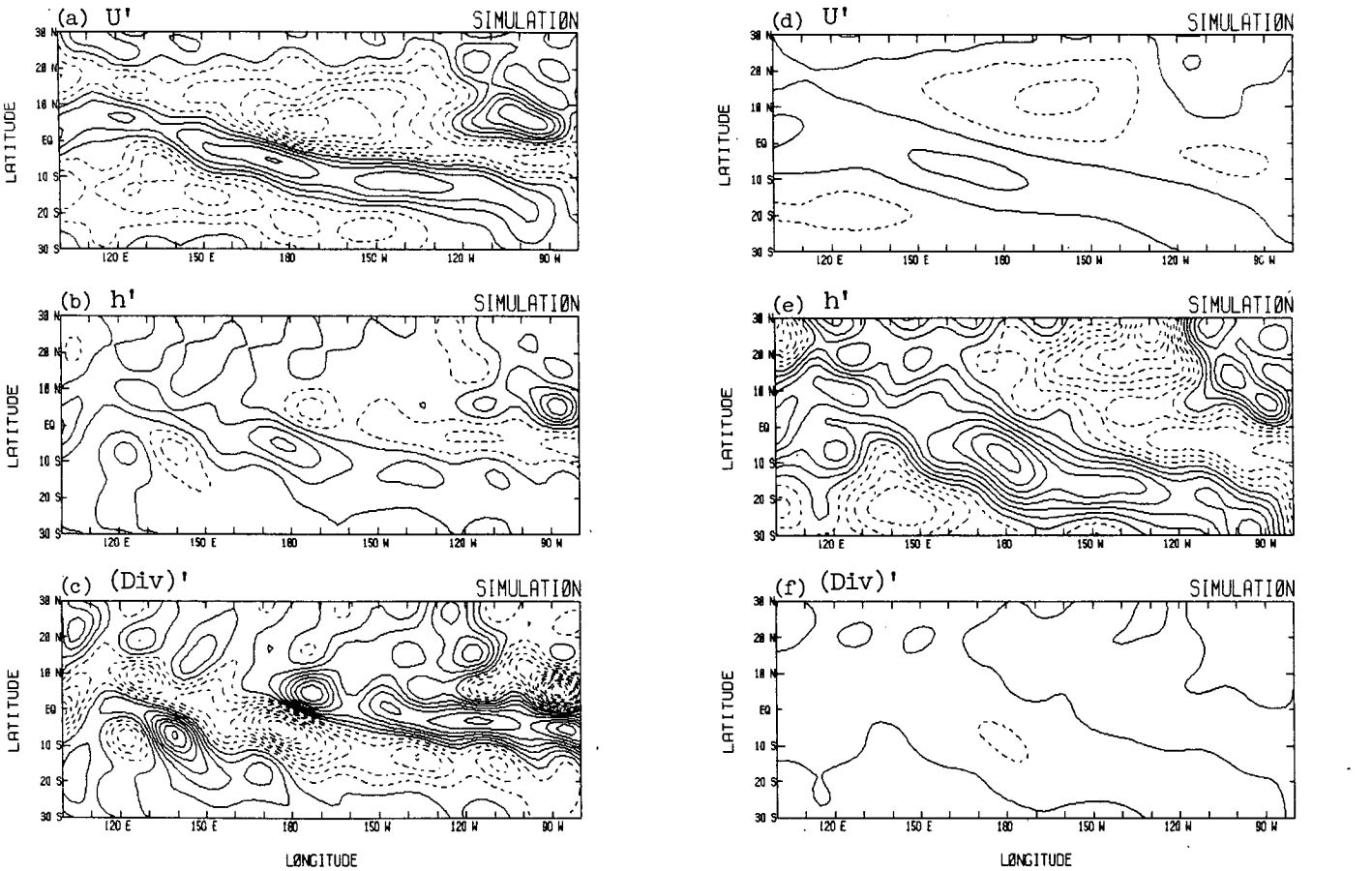


FIG. 10. The sensitivity of the summertime solutions to parameter $\tau_c$. The solutions shown in the left-hand panel are obtained with $\tau_c$ = 10 min. (a) $U'$, (b) $h'$, the eddy geopotential height of the trade inversion in our simple model, and (c) the eddy divergence; the contour intervals are 1 m s$^{-1}$, 2 gpm, and $4 \times 10^{-7}$ s$^{-1}$. The corresponding solutions in the right panel are obtained with $\tau_c$ = 3 h.

damping coefficient $\epsilon$ ($\equiv C_d|V_c|/H_0$) increases [from (2.5 days)$^{-1}$ to (1.666 days)$^{-1}$]; the new solution is, however, changed only a little: the tropical convergence is also identical, the $V'$ field is weaker by about 5% while the $U'$ field, the one most affected, is reduced by $\sim$35% in amplitude (in all cases, the phase is nearly unchanged). The above described weak dependence of the tropical solutions on $H_0$ is due to the neutralizing influence of the boundary layer height gradients on the imposed pressure gradient field.

## 5. The zonally symmetric model and solutions

In this section, we determine the component of the lower tropospheric Hadley circulation that is forced by the surface temperature distribution alone. As the upward and poleward transfer of westerly momentum from the region of tropical surface easterlies is accomplished in tropical latitudes mainly by the mean meridional circulation, the Hadley circulation in the tropical lower troposhere cannot be assumed to be uncoupled to the tropospheric circulation aloft. The zonally averaged tropical circulation being calculated in this section is therefore not the full solution as the influence of mid- and upper tropospheric Hadley circulation on the zonally symmetric tropical circulation beneath the trade inversion is simply ignored. It will, however, be shown that the "surface-forced" component of the solution determines, to a large extent, the total low-level convergence.

### a. *The zonally symmetric model*

The steady linear model for the zonally symmetric low-level tropical flow is obtained by retaining only the zonal mean terms during the linearization of the vertically averaged momentum equations that include the effects of the back pressure. The model equations are

$$f\bar{V} = \epsilon\bar{U} \tag{12a}$$

$$f\bar{U} = -\left[(2 - n\bar{T}_s + n\alpha H_0)\frac{\partial \bar{h}}{\partial \theta} - \frac{nH_0}{2}\frac{\partial \bar{T}_s}{\partial \theta}\right] - \epsilon\bar{V} \tag{12b}$$

$$\bar{h} = \frac{H_0\tau_c}{a\cos\theta}\left[\frac{\partial(\bar{V}\cos\theta)}{\partial\theta}\right], \tag{12c}$$

where the notation is as before, and $\epsilon$, $\tau_c$ and $H_0$ have the same values as in section 3. The meridional pressure gradient has a contribution from the north–south gradient of zonal mean surface temperature and also from the back pressure generated in this simple one-layer model by the modulation of the zonally averaged boundary layer height, $\bar{h}$. The zonal flow is forced directly whereas the mean meridional flow is frictionally driven; the interpretation of the model dynamics, in particular, of $\tau_c$ and $\bar{h}$, is much the same as in the case of the eddy model. The above equations are meridionally finite differenced using centered differencing of derivatives and solved in tandem on a latitudinal grid of grid size $\Delta\theta = 1°$; the boundary conditions are simply that $\bar{U} = \bar{V} = \bar{h} = 0.0$ at $\theta = \pm 90°$.

### b. *Zonal mean solutions*

The solutions obtained for FGGE summer are shown in Figs. 11a–c; to facilitate comparison, the corresponding ECMWF analyzed FGGE fields are shown in the same figures using the dashed line. Zonally symmetric solutions and "observations" for the FGGE winter are shown in the right-hand panel in Figs. 11d–f. As evident from Fig. 11, the zonally symmetric zonal flow, $\bar{U}$, calculated using the above model, is considerably different from the corresponding ECMWF analyzed fields, particularly, in the subtropics and extratropics of the winter hemisphere. The mechanism proposed in this section was not supposed to model the total low-level zonally averaged flow but only that part of it that is forced from below by the surface temperature gradients, and therefore discrepancies between the model solutions and the ECMWF analyzed fields (or for that matter any other analysis of the same dataset) are to be expected. It is, however, noteworthy that the proposed simple model is able to capture a significant fraction of the total zonal-mean meridional flow and divergence; the model is also able to simulate many of the interseasonal variations, e.g.,

- The latitudinal displacement of the convergent maximum (or the ITCZ) with seasons is well simulated; during summer, this maximum is located at ~10°N while during winter, it is at ~4°N, much like what is seen in the ECMWF analyzed product.
- The low-level meridional flow is rather well simulated during FGGE summer; $\bar{V}$ changes sign at ~17°N and the northward flow is much more robust in comparison with the equatorward flow from the Northern Hemispheric extratropics much as observed. During winter, the situation is just the opposite both in the model solutions and FGGE observations: the equatorward flow from the north is now stronger than the poleward flow from the south with the transition occurring within a few degrees of the equator.
- Indicated in the low-level solutions is (i) a strong southern hemispheric Hadley cell which extends well into northern latitudes and overshadows the Northern Hemisphere cell during northern summer, and (ii) a Northern Hemispheric Hadley cell which, during northern winter, is stronger than the southern hemispheric counterpart and which is contained essentially in the Northern Hemisphere. These indications are present also in the ECMWF analyzed FGGE observations except that the low-level convergence maximum during northern summer, instead of being greater, is in fact diagnosed to be smaller than the similar maximum during northern winter. This may, possibly, be an artifact of the adiabatic initialization schemes used in the ECMWF analysis rather than a real feature. We are computing similar quantities from the GFDL analysis which uses instead a diabatic initialization in the tropics.

It is worth noting that we have not tried to tune the zonal-mean model in any manner; except for the differences noted already, the dynamics governing the zonally symmetric part of the flow should not be any different from that governing the eddy flow, and so we have used the same parameter values as in section 3. Extensive tuning seemed unjustified given the imperfections in the analyses schemes. Also, if our simple model is capable of determining a significant fraction of the zonal-mean divergence, then the remaining forcing of the low-level zonally symmetric flow (presumably due to a stress from above) will result in corrections that are nearly divergence free (or rotational).

## 6. Summary and conclusions

We set out to determine the potential contribution of the SST gradient-driven flow to the *low-level* convergence over tropical oceans, and in case the contribution turned out to be significant, to ascertain to what extent this mechanism could explain the observed distribution of precipitation. Our emphasis has been on the convergence produced by sea surface temperature distributions rather than on the explicit thermodynamic effects of the sea surface temperature. The latter was emphasized by Neelin and Held (1987) who used the concepts of moist static energy and moist static stability to interpret the relationship between SST and tropical convergence.

The essential underlying assumption made in this investigation, and corroborated to an extent by the ECMWF analyzed FGGE data, is that the sea surface temperature and its gradients are correlated positively in the vertical through the depth of the trade cumulus layer which is taken to be 3 km deep. We ignore the influence of atmospheric motions or pressure gradients above the trade inversion on the flow beneath it (in the context of our simple one-layer model this was equivalent to having the layer topped by an almost flat isobaric surface). Riehl (1979) was, perhaps, the first one to explore the implications of such assumptions; in a limited study, he tried to understand and relate the observed temperature gradient in the eastern Pacific

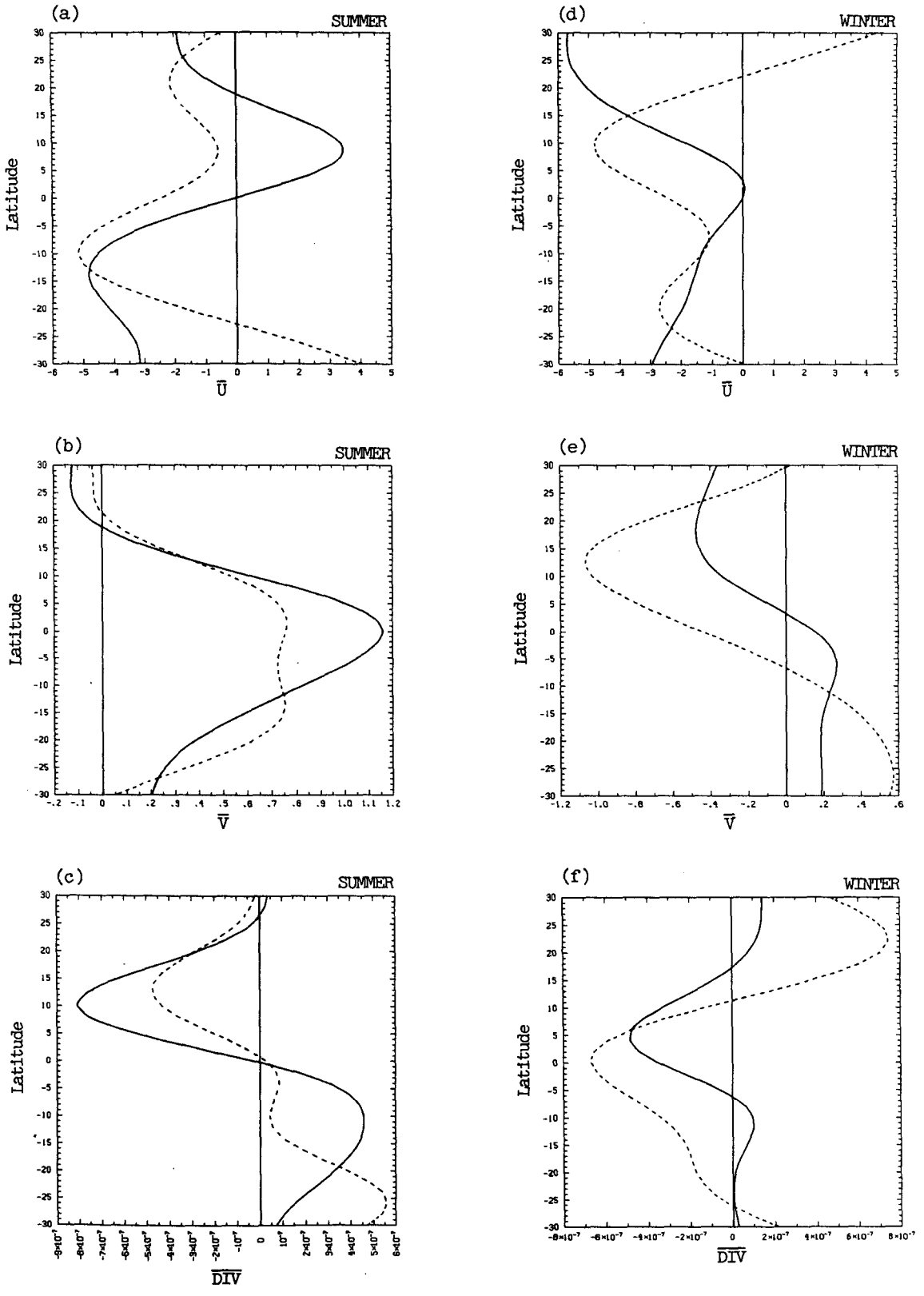


FIG. 11. The low-level zonally symmetric circulation obtained using the model described in section 5 is shown for the FGGE summer in the left panel. The dashed line in each figure is a smoothed version of the corresponding ECMWF analyzed field; shown are (a) $\bar{U}$, (b) $\bar{V}$, and (c) the zonally symmetric divergence. The corresponding wintertime solutions are shown in the right-hand panel.

trade cumulus layer along the California–Hawaii air–sea route to the observed sea-level pressure gradient.

Our study has demonstrated the importance of taking account of the fact that cumulonimbus convection takes a small but finite time to adjust to low-level convergence. When we failed to allow for this we obtained unreasonably large equatorial convergence. Allowing for this prevented large flows and convergences by permitting the low-level flow to modestly redistribute mass. Within our simple model this took the form of allowing undulations in the thickness of our boundary layer. These undulations—though very important—amounted to less than 10 gpm.

The model solutions compare more favorably with the ECMWF analyzed FGGE fields during summer than in winter for reasons discussed in section 3. We are currently in the process of comparing the model solutions against the GFDL FGGE analyses as well, because different analysis schemes can produce considerably different end products, particularly, in the tropics. Lau (1984), for example, compared the divergent component of the tropical wind analyses produced by GFDL and ECMWF, and found the monthly mean analyses to differ by as much as 50%. Seigel (1985) made intercomparisons of the surface wind analyses produced by ECMWF and NMC during 1982–83, and found the analyzed monthly mean zonal winds over tropical oceans to differ by as much as 3 m $s^{-1}$. Because of such differences, detailed comparisons with ECMWF FGGE analyses are probably unwarranted. While the degree of correspondence is encouraging, all we can say with certainty is that a very large part of tropical moisture convergence (which in turn determines the distribution of precipitation) is, in fact, forced by the surface temperature distribution.

In summary, we find:

(i) The sea surface temperature along with its gradients is an important forcing mechanism of the low-level tropical flow and convergence. The low-level forcing in our calculations results from differential heating of the trade cumulus layer, and not to any net latent heat release.

(ii) A reasonable description of the low-level tropical flow ($U'$, $V'$ and $\nabla_h \cdot \mathbf{V}'$) is obtained using the above described forcing mechanism only if the cumulonimbus mass flux exiting through the trade inversion is allowed to adjust to the horizontal convergence over a finite time (30 minutes or so). An instantaneous adjustment in which the trade inversion height remains flat leads to very unrealistic flow as does a slow adjustment (adjustment time greater than an hour). This has important implications for cumulus parameterization.

(iii) Although forcing by SST gradients is not able to well simulate the zonally symmetric zonal flow ($\bar{U}$), presumably due to the neglect in our model of the effects of any stresses on the low-level zonally symmetric circulation from the Hadley circulation above the trade inversion, it does well in simulating the other fields: the zonal mean meridional wind ($\bar{V}$) and the "all important" axially symmetric convergence.

(iv) Although zonal SST gradients are smaller than the meridional SST gradients over the tropical Pacific during the FGGE summer, the former are comparably important in forcing the low-level tropical circulation and convergence especially in the vicinity of the SPCZ.

(v) The momentum balance in the model's tropics continues to be essentially geostrophic within a few degrees of the equator, and this is true even in the presence of a Rayleigh friction coefficient as large as $(2.5 \text{ days})^{-1}$.

(vi) The net eddy tropical convergence in our model has important contributions from several terms. Both the Laplacian of the effective pressure field and the contribution due to latitudinal variation of the Coriolis parameter are big, comparable, and largely compensating. Another decomposition of the net convergence into geostrophic and frictional parts indicates that geostrophic convergence too is large (three times the net convergence in places) in the tropics except right at the equator. Because the net convergence is not easily relatable to the Laplacian of the effective pressure field alone, which would have been the case if horizontal momentum balance was essentially frictional, there is no obvious reason to always expect precise spatial coincidence of warm SSTs and tropical precipitation even though our results do corroborate this relationship.

(vii) In spite of sufficient Rayleigh damping, the tropical flow is extremely sensitive to the near-equatorial pressure gradients especially in models in which the pressure field is prescribed, i.e., not allowed to respond/adjust to the horizontal convergence of mass (as in section 2). When a coarse latitudinal grid is used, the sensitivity of the numerical solutions is somewhat reduced due to the implicit meridional smoothing of the forcing fields.

(viii) When modeling tropical flow and convergence, it is important to ensure that the convergence, too, be simulated correctly as this field is more sensitive to any model imperfections than the horizontal velocity fields. Moreover, the tropical low-level convergence (together with evaporation) determines precipitation which is likely to be better measured than the velocity fields themselves (at least over land); and so, a suitable simulation of tropical convergence is essential for validation of any tropical model.

Finally, we should note that our present results suggest the possibility that airflow over tropical oceans is largely determined by the distribution of sea surface temperature. If this is the case, our model provides a simple parameterization of the atmosphere for ocean models wherein air–sea interaction is important.

*Acknowledgments.* The authors wish to acknowledge support from NASA Grant NAGW-525 and NSF grants ATM-8342482 and ATM-8520354.

## APPENDIX A

### Derivation of Equation for Fluctuations in $Z_T$

Let $M'_c$ be that portion of the cumulus mass flux associated with low-level convergence. From (8)

$$M'_c = -\int_0^{Z_T} \nabla \cdot \rho \mathbf{V} dz = -\frac{H_0 \rho}{a \cos\theta}\left[\frac{\partial U'}{\partial \lambda} + \frac{\partial (V' \cos\theta)}{\partial \theta}\right]. \tag{A1}$$

While this equation is correct for the steady state, it does not include the fact that it takes a finite, nonzero time for $M'_c$ to adjust to the low-level convergence. The following obvious modification to (A1) allows for this adjustment time:

$$\tau_c \frac{\partial}{\partial t} M'_c + M'_c = -\frac{H_0 \rho}{a \cos\theta}\left[\frac{\partial U'}{\partial \lambda} + \frac{\partial (V' \cos\theta)}{\partial \theta}\right], \tag{A2}$$

where $\tau_c$ is adjustment time.

At the same time, the continuity equation tells us that at any instant the horizontal mass convergence must be balanced by the cumulus mass flux out of the layer, $M'_c$, and the time rate of change of the column density of the layer, $\rho \partial h'/\partial t$; i.e.,

$$\rho \frac{\partial h'}{\partial t} + M'_c = -\frac{H_0 \rho}{a \cos\theta}\left[\frac{\partial U'}{\partial \lambda} + \frac{\partial (V' \cos\theta)}{\partial \theta}\right]. \tag{A3}$$

Comparing (A3) and (A2) we see that

$$h' = \frac{\tau_c M'_c}{\rho}. \tag{A4}$$

In equilibrium, $\partial/\partial t = 0$, and $M'_c$ is given by (A1). Equation (A4) then yields (10) in the text, namely

$$h' = -\tau_c \frac{H_0}{a \cos\theta}\left[\frac{\partial U'}{\partial \lambda} + \frac{\partial (V' \cos\theta)}{\partial \theta}\right]. \tag{A5}$$

## APPENDIX B

### Method of Obtaining Eddy Solutions

The eddy dynamical model is solved using a semi-spectral approach in which the zonal Fourier representation is truncated at wavenumber 15, e.g.,

$$h'(\lambda, \theta) = \sum_{m=1}^{15} 2\,\mathrm{Re}[\tilde{h}_m(\theta) \exp(im\lambda)],$$

where $\tilde{h}_m(\theta)$ is the complex amplitude associated with the $m$th zonal wavenumber; all other eddy fields are similarly represented. Both the eddy and the zonal mean equations are finite-differenced on a meridional grid having 181 equally spaced grid points between the two poles (i.e., $\Delta\theta = 1°$). When solving either of the models, the three finite difference equations are solved in tandem by inverting block tridiagonal matrices using the following boundary conditions:

$$\tilde{U}_m = \tilde{V}_m = \tilde{h}_m = 0.0 \quad \text{at} \quad \theta = \pm 90° \quad \text{for all m.}$$

## REFERENCES


Albrecht, B. A., A. K. Betts, W. H. Schubert and S. K. Cox, 1979: A model of the thermodynamic structure of the trade-wind boundary layer. Part I: Theoretical formulation and sensitivity tests. *J. Atmos. Sci.*, **36**, 73–79.

Augstein, E., H. Schmidt and F.Ostapoff, 1974: The vertical structure of the atmospheric boundary layer in undisturbed trade winds over the Atlantic Ocean. *Bound.-Layer Meteor.*, **6**, 129–150.

Betts, A. K., 1973: Nonprecipitating cumulus convection and its parameterization. *Quart. J. Roy. Meteor. Soc.*, **99**, 178–196.

Burpee, R. W., and R. J. Reed, 1982: Synoptic-scale motions. The GARP Atlantic Tropical Experiment (GATE) Monogr., GARP Publ. Ser. No. 25, April 1982, WMO/ICSU, 61–120.

Charney, J. G., and A. Eliassen, 1964: On the growth of the hurricane depression. *J. Atmos. Sci.*, **21**, 68–75.

Cornejo-Garrido, A. G., and P. H. Stone, 1977: On the heat balance of the Walker circulation. *J. Atmos. Sci.*, **34**, 1155–1162.

Geisler, J. E., 1981: A linear model of the Walker circulation. *J. Atmos. Sci.*, **38**, 1390–1400.

Gill, A. E., 1980: Some simple solutions for heat induced tropical circulations. *Quart. J. Roy. Meteor. Soc.*, **106**, 447–462.

——, and P. J. Phlips, 1986: Nonlinear effects on heat-induced circulation of the tropical atmosphere. *Quart. J. Roy. Meteor. Soc.*, **112**, 69–91.

Held, I. M., and A. Y. Hou, 1980: Nonlinear axially symmetric circulation in a nearly inviscid atmosphere. *J. Atmos. Sci.*, **37**, 515–533.

Horel, J. D., 1982: On the annual cycle of the tropical Pacific atmosphere and ocean. *Mon. Wea. Rev.*, **110**, 1863–1878.

Kuo, H. L., 1965: On formation and intensification of tropical cyclones through latent heat release by cumulus convection. *J. Atmos. Sci.*, **22**, 40–63.

Lau, N.-C., 1984: A comparison of circulation statistics based on FGGE level III-B analyses produced by GFDL and ECMWF for the special observing periods. NOAA Data Rep. ERL GFDL-6.

Liebmann, B., and D. L. Hartmann, 1982: Interannual variations of outgoing IR associated with tropical circulation changes during 1974–78. *J. Atmos. Sci.*, **39**, 1153–1162.

Lindzen, R. S., 1981: Some remarks on cumulus parameterization. *Proc. of the NASA Cloud, Climate Conf.*, NASA Report. [Available from the NASA/Goddard Institute of Space Studies.]

——, B. Farrell and A. J. Rosenthal, 1982: Absolute barotropic instability and monsoon depressions. *J. Atmos. Sci.*, **40**, 1178–1184.

Neelin, J. D., and I. M. Held, 1987: Modeling tropical convergence based on the moist static energy budget. *Mon. Wea. Rev.*, (in press).

Neiburger, M., D. S. Johnson and C. W. Chien, 1961: Studies of the structure of the atmosphere over the eastern Pacific Ocean. I: The inversion over the eastern north Pacific Ocean. University of California Press, 94 pp.

Ooyama, K., 1969: Numerical simulation of the life cycle of tropical cyclones. *J. Atmos. Sci.*, **26**, 3–40.

Ramage, C. S., and A. M. Hori, 1981: Meteorological aspects of the El Niño. *Mon. Wea. Rev.*, **109**, 1827–1835.

Rasmusson, E. M., and T. H. Carpenter, 1982: Variations in tropical sea surface temperature and surface wind fields associated with the Southern Oscillation/El Niño. *Mon. Wea. Rev.*, **110**, 354–384.

Riehl, H., 1979: The trade wind inversion. *Climate and Weather in the Tropics.* Academic Press, 611 pp.

Rosenlof, K. H., D. E. Stevens, J. R. Anderson and P. E. Ciesielski, 1986: The Walker circulation with observed zonal winds, a mean Hadley cell, and cumulus friction. *J. Atmos. Sci.*, **43**, 449–467.

Sarachik, E. S., 1985: A simple theory for the vertical structure of the tropical atmosphere. *Pure Appl. Geophys.*, **123**, 261–271.

Schneider, E. K., 1977: Axially symmetric steady-state models of the basic state for instability and climate studies. Part II: Nonlinear calculations. *J. Atmos. Sci.*, **34**, 280–296.

——, and R. S. Lindzen, 1977: Axially symmetric steady-state models of the basic state for instability and climate studies. Part I: Linearized calculations. *J. Atmos. Sci.*, **34**, 263–279.

Seigel, A. D., 1985: Comparisons of the NMC, ECMWF, and FNOC low-level wind fields during 1982–83. *Proc. of the First WMO Workshop on the Diagnosis and Prediction of Monthly and Seasonal Atmospheric Variations over the Globe,* College Park, MD.

Shukla, J., and J. M. Wallace, 1983: Numerical simulation of the atmospheric response to equatorial Pacific sea surface temperature anomalies. *J. Atmos. Sci.*, **40**, 1613–1630.

Stevens, D. E., and R. S. Lindzen, 1978: Tropical wave-CISK with a moisture budget and cumulus friction. *J. Atmos. Sci.*, **35**, 940–961.

——, R. S. Lindzen and L. J. Shapiro, 1977: A new model of tropical waves incorporating momentum mixing by cumulus convection. *Dyn. Atmos. Oceans,* **1**, 365–425.

Stone, P. H., and R. M. Chervin, 1984: The influence of ocean surface temperature gradient and continentality on the Walker circulation. Part II: Prescribed global changes. *Mon. Wea. Rev.*, **112**, 1524–1534.

Webster, P. J., 1972: Response of the tropical atmosphere to local steady forcing. *Mon. Wea. Rev.*, **100**, 518–541.

Wu, J., 1980: Wind stress coefficients over sea surface near neutral conditions—A revisit. *J. Phys. Oceanogr.*, **10**, 727–740.

Zebiak, S. E., 1982: A simple atmospheric model of relevance to El Niño. *J. Atmos. Sci.*, **39**, 2017–2027.